Experimental study of chirp effect on supercontinuum generation in photonic crystal fibers

Yongliang Jiang (姜永亮), Bing Zhou (周 冰), Yuxin Leng (冷雨欣), Xiaoyan Liang (梁晓燕), and Zhizhan Xu (徐至展)

State Key Laboratory of High Field Laser Physics, Shanghai Institute of Optics and Fine Mechanics, Chinese Academy of Sciences, Shanghai 201800

The chirp effect in supercontinuum (SC) generation in photonic crystal fibers (PCFs) is researched carefully in experiment. Using an acoustic-optics programmable dispersive filter (AOPDF), the 1−4 order dispersions of the pulses from femtosecond oscillator can be accurately controlled. The experimental results show the SC generation in PCF is sensitive to the chirp of incident pulse, and the output spectrum and conversion efficiency can be tuned by changing the initial dispersion state. With different group delay dispersion (GDD) brought to the incident pulse, we find that positive chirp can enhance the energy conversion to long wavelength, and negative chirp can enhance the conversion to short wavelength. Specially, an optimal negative chirp can maximize the conversion to the shortest one at about 625 nm. The effect of the third-order dispersion (TOD) also has been investigated, and we find that the same value of the positive and negative TOD has the similar effect on the SC.

OCIS codes: 140.3510, 320.7110, 300.6420, 320.1590.

Since the first observation in the late 1960s[1], the phenomenon of supercontinuum (SC) generation has been demonstrated in a variety of materials, including solids, liquids[2], and gases[3,4]. Over the past several years, all-silica photonic crystal fiber (PCF) with high nonlinear coefficient has been proved to be an effective instrument to produce reliable SC with low pump energy. With the same input pulse, the output SC can be controlled by customizing the fiber dispersion profile, which is impossible for classical fibers. A SC covering more than two octaves has been generated in several centimeters of PCF using ultra-short fs pulses from an oscillator[5]. Such SC sources can be used in many applications, such as optical coherence tomography (OCT)[6] and optical frequency metrology[7], etc.. SC generation in PCF with ultra-short pulses has become a subject of great interest worldwide.

Many numerical and experimental studies have been carried out to analyze the influence of the input pulse properties such as peak power, pulse duration, central wavelength, etc. The initial chirp of the input pulse has been theoretically predicted to have a great influence on the SC generation[8]. However, to our knowledge, the effects of initial chirp, especially high-order phase distortions, have not been experimentally studied in detail. Using an acousto-optic programmable dispersive filter (AOPDF), the 1−4 order dispersions of the pulses from femtosecond oscillator can be accurately controlled[9]. Here we present the detailed experimental study how the 2nd and 3rd order phase distortions affect the SC generation in PCFs.

Ultra-short pulses generation in PCF is a complex process, and there are several nonlinear processes responsible for the SC generation, such as self-phase modulation (SPM), self-steepening, and stimulated Raman scattering (SRS), etc.. Without considering the polarization coupling[10], a generalized scalar nonlinear Schrödinger equation can be used to describe the ultra-short pulse propagation inside the PCF[8]:

$$\frac{\partial A}{\partial z} = \sum_{m\geq 2} \frac{i^{m+1}}{m!} \frac{\partial^m A}{\partial \tau^m} - \frac{\alpha}{2} A + i\gamma \left(1 + \frac{i}{\omega_0} \frac{\partial}{\partial \tau}\right) \times \left[A(z,\tau) \int_{-\infty}^{\tau} d\tau' R(\tau - \tau') |A(z,\tau')|^2\right], \quad (1)$$

where A is the electric-field amplitude, z is the longitudinal coordinate along the fiber, τ is the time in a reference frame traveling with the pump light, β_m is the mth-order dispersion coefficient at the central frequency ω_0, α is the fiber loss, $\gamma = n_2\omega_{0/(cA_{\rm eff})}$ is the nonlinear coefficient, $n_2 \approx 2.0 \times 10^{-20}$ m^2/W is the nonlinear refractive index of fused-silica glass, and $A_{\rm eff}$ is the effective mode area of the fiber.

The response function $R(\tau) = (1 - f_{\rm R})\delta(\tau) + f_{\rm R} h_{\rm R}(\tau)$ includes both instantaneous electronic and delayed Raman contributions. Here $f_{\rm R} = 0.18$ is the fraction of the Raman contribution to the nonlinear polarization, and $h_{\rm R}(\tau)$ is the Raman response function of silica fiber, which can be approximately expressed as $h_{\rm R}(\tau) = (\tau_1^2 + \tau_2^2)/(\tau_1\tau_2^2)\exp(-\tau/\tau_2)\sin(\tau/\tau_1)$, where $\tau_1 = 12.2$ fs and $\tau_2 = 32$ fs[11,12].

The nonlinear Schrödinger equation allows for modeling the propagation of pulses with spectral width comparable to the central frequency ω_0. By including enough high-order dispersion terms, this equation can be used to simulate few-cycle pulses[12]. Equation (1) can be numerically solved by using the split-step Fourier method.

The experimental setup is shown in Fig. 1. A laser diode-pumped femtosecond oscillator generates a 75-MHz train of 9-fs pulses with 592-mW average power at 800-nm center wavelength, and the full width at half maximum (FWHM) is about 200 nm. An AOPDF was employed after the oscillator to manipulate the chirp of the pump pulses for SC generation. After the selection and modulation of AOPDF, only 1000 Hz fractions of the pulse train are selected and the FWHM is reduced to 80 nm (Fig. 2). The pulse energy will be attenuated by the filter with a diffraction efficiency of about 50%. The

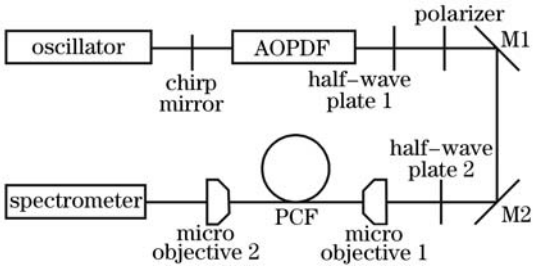

Fig. 1. Experimental setup.

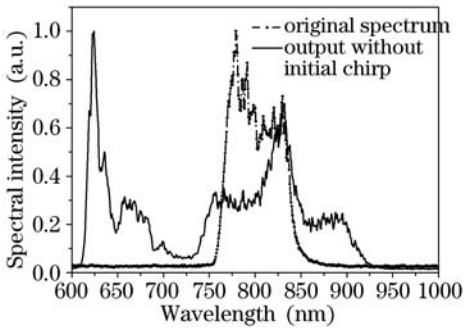

Fig. 2. Spectra of the input pulse and output without initial chirp.

FWHM of temporal width after AOPDF is measured to be about 20 fs by an autocorrelator.

The pump power can be controlled by the half-wave plate and polarizer after AOPDF, and another half-wave plate is employed to manipulate the pump polarization state. A 40× micro-objective with a numerical aperture of NA=0.65 is used to couple the pump pulses into the PCF, and another 20× micro-objective is used to collimate the output pulses. The typical average power before micro-objective is measured to be 65 mW.

The PCF used in our experiment is a commercial one (Crystal Fibre A/S) with a length of 20 cm. It has a zero dispersion around 750 nm with a high nonlinear coefficient of $\gamma = 95\ (\mathrm{W \cdot km})^{-1}$. The fiber is polarization maintaining.

The spectra in this experiment are all measured by a portable fiber spectrometer (USB2000, Oceanoptics). Limited by the detection range of the spectrometer, the spectral part with a wavelength longer than 1100 nm cannot be effectively measured.

When the AOPDF is set to self-compensation state, the dispersion of the acousto-optic crystal can be well compensated, which means that the chirp state of the pump pulse has not been changed. The original spectra and the corresponding SC spectra without chirp effect are compared in Fig. 2. The observed SC can be separated to two parts from the zero-dispersion wavelength: long-wave part and short-wave part. And each part comprises of a series of discrete peaks. The short-wave part comprises of three obvious peaks: 625, 665 and 700 nm, and the peaks of the long-wave part are located at 760, 830 and 890 nm separately.

The 2nd-order chirp effect was studied by changing the group delay dispersion (GDD) parameter of the AOPDF. From Fig. 3 we can see that the SC profile is sensitive to the 2nd-order phase distortion. With different GDD

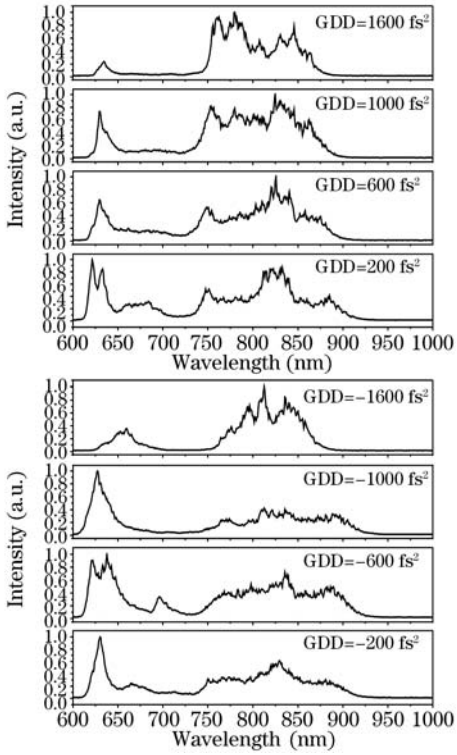

Fig. 3. Effect of GDD on the output SC.

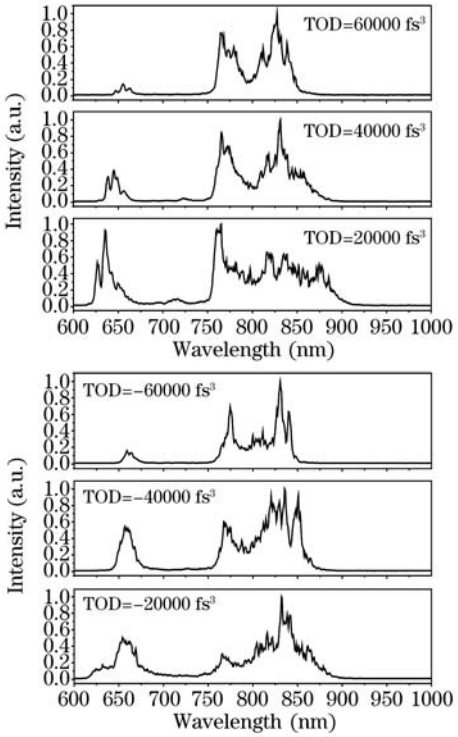

Fig. 4. Effect of TOD on the output SC.

brought to the pump pulse, we find that an optimal positive chirp can enhance the energy conversion to long-wave part and an optimal negative chirp can enhance the conversion to short-wave part, which is instructive when we want to acquire maximal conversion to a specific

wavelength. For example, a negative chirp of about -1000 fs^2 can maximize the conversion to the shortest peak at about 625 nm, and a negative chirp of about -600 fs^2 can maximize the peak at 700 nm. An optimal positive chirp of about 300 fs^2 can maximize the conversion to the peak at about 830 nm. When the absolute value of the GDD is too large the conversion efficiency will be too poor to acquire bandwidth large enough due to low peak power.

The 3rd-order chirp effect also has been investigated in the same way. By changing the 3rd-order dispersion (TOD) parameter of AOPDF, we find that our SC profile is not sensitive to 3rd-order phase distortion, and the same value of positive and negative TODs has the similar effect on the SC, as shown in Fig. 4. With the increase of the absolute value of TOD, the SC gets weak due to the decreasing peak power.

In conclusion, with an AOPDF, we have experimentally studied the chirp effects of the pump pulse on the SC generation in PCF. We find that the output spectrum and conversion efficiency can be tuned by changing the initial chirp state. The SC profile is sensitive to the change of 2nd-order phase distortion and not sensitive to the 3rd-order phase distortion. An optimal positive GDD will enhance the energy conversion to long-wave part and an optimal negative GDD will enhance the conversion to short-wave part. The same value of positive and negative TODs has the similar effect on the SC. When the absolute value of the chirp is too large the conversion efficiency will be too poor to acquire SC generation due to low peak power.

This work was partially supported by the National Natural Science Foundation of China (No. 10576012 and 60538010), the National High-Technology Research and Development Program of China (No. 2004AA84ts12), and the Specialized Research Fund for the Doctoral Program of Higher Education of China (No. 20040532005). Y. Jiang's e-mail address is jiangyongliang@siom.ac.cn.

References

1. R. R. Alfano and S. L. Shapiro, Phys. Rev. Lett. **24,** 584 (1970).
2. R. L. Fork, C. V. Shank, C. Hirlimann, and R. Yen, Opt. Lett. **8,** 1 (1983).
3. P. B. Corkum, C. Rolland, and T. Srinivasan-Rao, Phys. Rev. Lett. **57,** 2268 (1986).
4. F. A. Ilkov, L. Sh. Ilkova, and S. L. Chin, Opt. Lett. **18,** 681 (1993).
5. J. K. Ranka, R. S. Windeler, and A. J. Stentz, Opt. Lett. **25,** 25 (2000).
6. I. Hartl, X. D. Li, C. Chudoba, R. K. Ghanta, T. H. Ko, J. G. Fujimoto, J. K. Ranka, and R. S. Windeler, Opt. Lett. **26,** 608 (2001).
7. R. Holzwarth, T. Udem, T. W. Hansch, J. C. Knight, W. J. Wadsworth, and P. St. J. Russel, Phys. Rev. Lett. **85,** 2264 (2000).
8. Z. Zhu and T. G. Brown, Opt. Express **12,** 689 (2004).
9. F. Verluise, V. Laude, Z. Cheng, Ch. Spielmann, and P. Tournois, Opt. Lett. **25,** 575 (2000).
10. Z. Zhu and T. G. Brown, J. Opt. Soc. Am. B **21,** 249 (2004).
11. A. L. Gaeta, Opt. Lett. **27,** 924 (2002).
12. A. L. Agrawal, *Nonlinear Fiber Optics* (3rd edn.) (Academic, San Diego, 2002).